Inorganic Chemistry, Vol. 56, No. 6 (2017): 3302-3309. DOI.

Contents

Redox and Spectroscopic Properties of Iron Porphyrin Nitroxyl in the Presence of Weak Acids

Md. Hafizur Rahman
Marquette University Chemistry Department, Milwaukee, WI
Michael D. Ryan
Marquette University Chemistry Department, Milwaukee, WI

Synopsis

Using voltammetric and chemical methods, Fe(OEP) (HNO) was generated and studied using visible, infrared, and NMR spectroscopy. The voltammetric and spectroelectrochemical data showed that this complex could be further reduced to Fe(OEP)(H_2NOH) or oxidized back to Fe(OEP) (NO). Further protonation of Fe(OEP) (HNO) was not observed.

Abstract

The spectroelectrochemistry and voltammetry of Fe(OEP) (NO) in the presence of substituted phenols was studied. Cyclic voltammetry showed that two closely spaced waves were observed for the reduction of Fe(OEP) (NO) in the presence of substituted phenols. The first wave was a single electron reduction under voltammetric conditions. The second wave was kinetically controlled, multielectron process. Visible spectroelectrochemistry of Fe(OEP) (NO) in the presence of substituted phenols showed that three species were present during the electrolysis. Additional spectroscopic studies indicated that the two reduction species were Fe(OEP) (HNO) and Fe(OEP)(H_2NOH). The Fe(OEP) (HNO) species, which can be generated chemically, was stable over a period of hours. Additional acid did not lead to further

protonation. Proton NMR spectroscopy confirmed the Fe(OEP) (HNO) species could be deprotonated under basic conditions. The third species, Fe(OEP)(H_2NOH), was generated by the further reduction of the chemically generated Fe(OEP) (HNO) complex. Both the Fe(OEP) (HNO) and Fe(OEP)(H_2NOH) complexes could be slowly oxidized back to Fe(OEP) (NO). At millimolar concentrations of Fe(OEP) (HNO), there was no evidence for the disproportionation of Fe(OEP) (HNO) to Fe(OEP) (NO) and H_2 in the presence of substituted phenols. Nor was there evidence for the generation of N_2O. The FTIR spectroelectrochemistry showed changes in the infrared spectra in the presence of substituted phenols, but no isotopic sensitive bands were observed for the reduced species between 1450 and 1200 cm^{-1}. This may be because the ν_{NO} band shifted into a region (1500–1450 cm^{-1}) where it would be difficult to observe.

Introduction

The formation of HNO complexes with iron porphyrins has been implicated in a large number of physiological and pathological processes,[1] including cytochrome *c* nitrite reductases (ccNiR),[2,3] fungal cytochrome P450 nitric oxide reductase (P450nor),[4,5] and hydroxylamine oxidoreductase.[6] The formation of ferrous nitroxyl (NO^- or HNO) has been postulated in the reduction of NO to N_2O by cytochrome P450nor.[7] DFT calculations have shown that the Fe(II)–NO^- complex is basic and can be protonated, at least with appropriate heme ligation.[8,9] The coordination chemistry of HNO with hemes has been reviewed by Farmer and Sulc,[10] while Speelman and Lehnert[11] examined the differences between heme and nonheme iron nitroxyl complexes. For heme complexes, the reduction of the Fe(P) (NO) complex (where P = porphyrin) was centered on the nitrosyl group,[12] which made that moiety quite basic. Lin and Farmer[13] reported the synthesis and characterization of a HNO complex with myoglobin. Farmer et al. used NMR, X-ray absorption, and resonance Raman spectroscopy for additional studies of this complex.[14,15] A ν_{NO} vibration of 1385 cm^{-1} was reported using resonance Raman spectroscopy, close to the ν_{NO} for the Ru(P) (HNO) complex (P = porphyrin).[16] Czarnecki and Kincaid used cryoradiolysis to obtain the low-wavenumber resonance Raman spectrum of the myoglobin Fe–HNO complex.[17] The visible spectrum of a Fe(PF) (HNO) complex (where PF was a picket-fence porphyrin) was reported by Goodrich et al.[18] A recent report by Abucayon et al.[19] showed the formation of an Fe(OEP) (HNO) (Im) (OEP = octaethylporphyrin) complex by hydride attack on the ferric nitrosyl complex. A similar approach had been used earlier in the formation of a Ru(P) (HNO) (Im) complex.[16] Spectroscopic properties (e.g., NMR, IR/Raman) of metalloporphyrin–HNO complexes were calculated using DFT and compared to experimental values by Ling et al.[20] Conradie and Ghosh[21] carried out DFT calculations on metal porphyrin–HNO complexes and found that the Fe(P) (HNO) complex was a low-spin ferrous complex. Cobalt and manganese complexes, though, yielded two low energy states.

The Fe(P) (HNO) complex in aqueous solutions has limited stability because there are a number of decomposition pathways. The reaction of HNO with metalloporphyrins was reviewed recently by Doctorovich et al.[22] In aprotic solvents, iron porphyrin–HNO complexes have been found decompose to Fe(P) (NO) and H_2.[18,23] This reaction though is slow with weak acids, and the work of Liu and Ryan[24] showed that this reaction was not important on the voltammetric time scale. Using weak acids such as substituted phenols, Fe(P) $(NO)^-$ reacted with phenol to generate Fe(P) (HNO).[24] The pK_a of a Ru-HNO complex with a nonporphyrin ligand was measured as 9.78 in aqueous solution, a value that is similar to or weaker than many substituted phenols.[25] At more negative potentials, the Fe(P) (HNO) complex can be further reduced to hydroxylamine (on the voltammetric time scale) and ammonia (on the

coulometric time scale).[24] Kinetic analysis of the reduction of Fe(P) $(NO)^-$ to Fe(P) (NH_2OH) indicated that the rate limiting step was the formation of a Fe(P)$(H_2NO)^+$ intermediate. On the basis of this work, the overall scheme for the reduction of Fe(P) (NO) in weak acids/nonaqueous solvents can be summarized in Scheme 1. In this scheme, the formation of Fe(P)$(H_2NO)^+$ was rate limiting step (reaction 4) but it was not clear if it was a significant species in solution at equilibrium. At the limiting current plateau for the second wave, where Fe(P) (NH_2OH) was formed, the current was consistent with the formation of $Fe^I(P)^-$[24] (reaction 5).

Scheme 1. Redox and Acid/Base Reactions for Fe(OEP) (NO) Species

$$\underset{(1)}{Fe(OEP)(NO)} + e^- \rightarrow \underset{(2)}{Fe(OEP)(NO)^-} \quad (1)$$

$$Fe(OEP)(NO)^- + PhOH \rightarrow \underset{(3)}{Fe(OEP)(HNO)} + PhO^- \quad (2)$$

$$Fe(OEP)(HNO) + 2\,e^- + 2\,PhOH \rightarrow \underset{(4)}{Fe(OEP)(H_2NOH)} + 2\,PhO^- \quad (3)$$

$$Fe(OEP)(HNO) + PhOH \rightarrow Fe(OEP)(H_2NO)^+ + PhO^- \quad (4)$$

$$Fe(OEP)(H_2NO)^+ + 3\,e^- + PhOH \rightarrow Fe(OEP)^- + H_2NOH + PhO^- \quad (5)$$

$$2\,Fe(OEP)(HNO) \rightarrow 2\,Fe(OEP)(NO) + H_2 \quad (6)$$

The Fe(P) (HNO) complexes that have been generated to date have used protected environments, such as proteins[13,26] or picket-fence porphyrins,[18] to prevent the decomposition of Fe(P) (HNO) to Fe(P) (NO) and H_2.[18,23] The voltammetric evidence though shows that this reaction is not fast, as it cannot be observed on the voltammetric time scale. Since metal coordinated nitroxyls are reasonably good bases (pK_a ≈ 9–10), even fairly weak acids, such as substituted phenols, can protonate this species, especially if the reaction is driven with an excess of acid. Under these conditions, it should be possible to observe the spectroscopic and chemical properties of Fe(P) (HNO) using spectroelectrochemistry.

Experimental Section

Chemicals

Tetrabutylammonium perchlorate (TBAP), iron(III) octaethylporphyrin (FeOEPCl), 2,6-dichlorophenol, sodium methoxide, and hydroxylamine hydrochloride were purchase from Sigma-Aldrich Chemical Co. Deuterated phenols (3,5-dichlorophenol-d_3 and 3,5-dichlorophenol-d_4) were obtained from CDN Isotopes. TBAP was dried at 90 °C under a vacuum overnight before use. Anhydrous THF was refluxed in the presence of sodium metal and benzophenone until the solution was a persistent dark blue color. After purification, the solvent was collected under argon and stored in the glovebox. All phenols were purified by sublimation. The iron-porphyrin nitrosyl and nitroxyl complexes were synthesized by literature methods,[12,27] as were the phenolate salts.[24]

Instrumentation

The boron-doped diamond (BDD) electrode (3 mm diameter) was obtained from Windsor Scientific, Ltd. (Slough, UK). Spectroelectrochemical (SEC) experiments used a low-volume thin layer quartz glass cell

purchased from BAS Inc. A platinum mesh was used as the working electrode and a platinum wire was used as the auxiliary electrode. Potentials were measured relative to the $Ag/AgNO_3$ (in CH_3CN) reference electrode. The UV–visible spectra were recorded on a HP 8452A diode array spectrophotometer. The FTIR spectroelectrochemical cell was previously described.[28] The infrared spectra were obtained using 64 scans and 2 cm^{-1} resolution, recorded with a Thermo Nicolet-FTIR spectrophotometer (Model 670 Nexus) with a MCT detector. ^1H NMR measurements were performed using a Varian 400 MHz FT spectrometer.

Procedures

All solutions were prepared in the glovebox and sealed with Teflon tape. The argon gas flow was continued above the voltammetric solutions until the end of the experiment. The argon gas was presaturated with THF. UV–visible and FTIR spectroelectrochemical experiments were carried out using one of two methods depending upon the solution. For UV–visible spectra, a slow cyclic scan of the potential was sufficient to ensure complete electrolysis at each potential. For the FTIR (except as noted), potentials were chosen to be sufficiently negative to ensure complete electrolysis. The DFT calculations for the infrared and NMR spectra were calculated using the procedures described previously.[12]

Results and Discussion

Cyclic Voltammetry of Fe(OEP) (NO)

The cyclic voltammetry of Fe(OEP) (NO) in THF in the absence and presence of 2,6-dichlorophenol (dcp) is shown in Figure 1. In the absence of 2,6-dcp, a single wave was observed, and the electron transfer was chemically reversible, with an $E°$ value of −1.25 V vs $Ag/AgNO_3$ (Scheme 1, reaction 1). The large ΔE_p value can be mostly attributed to uncompensated solution resistance. With the addition of 10 mM 2,6-dcp, the wave shifted to more positive potentials and the oxidation peak decreased significantly, compared to the voltammetry in the absence of 2,6-dcp. This indicated that Fe(OEP) $(NO)^-$ reacted with the phenol. As the scan rate was decreased, the peak current ratio approached one as expected for a reversible chemical reaction (Figure S1). The increased chemical reversibility was consistent with an EC (reversible) mechanism (reactions 1–2, Scheme 1).

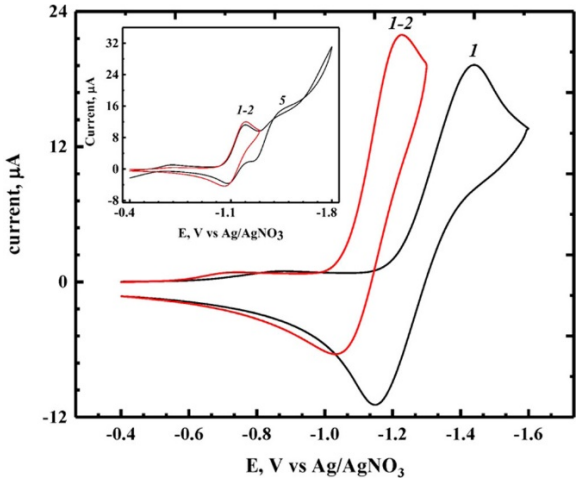

Figure 1. Cyclic voltammetry of 0.89 mM Fe(OEP) (NO) in THF with 0.10 M TBAP. Absence of 2,6-dcp (black line) and 10 mM 2,6-dcp (red line). Scan rate: 200 mV/s. Insert: 10 mM 2,6-dcp, Scan rate: 50 mV/s. Switching potential: −1.30 (red) and −1.80 V (black). BDD electrode. Italic numbers in figures refer to the reactions in Scheme 1.

The fact that the forward peak current increased minimally in the presence of 2,6-dcp indicated that the Fe(OEP) (HNO) complex was not further reduced under voltammetric conditions (a 10% increase in the peak current is consistent with an EC mechanism). In addition, the minimal increase in the peak current will also rule out the disproportionation reaction (reaction 6, Scheme 1) under voltammetric conditions as this would lead to a significant increase in the peak current. If the scan window was increased, a second wave was observed (Figure 1 insert). This wave was previously observed in polarography, and led to the formation of hydroxylamine (on the voltammetric time scale) and ammonia (on the coulometric time scale).[24] These results were consistent with the behavior that was previously reported on mercury using normal pulse polarography.[24] The kinetics of the second redox process was thoroughly examined in that work, and corresponded to a kinetically controlled 3-electron process. The current for the second wave was strongly dependent upon the scan rate and the acid concentration.[24] Three electrons were only observed at slow scan rates and/or high acid concentrations. Since reactions 4–5 (Scheme 1) have already been studied in detail, the focus of this work will be the characterization and reactivity of the intermediate species, Fe(OEP) (HNO).

Similar voltammetric behavior was observed for a series of phenols, including phenol itself, 2,3-dcp, 2,6-dcp and 3,5-dcp. The pK_a values of these acids are shown in Table 1. As the pK_a of the acid decreased, the concentration of the substituted phenol needed to shift the wave increased. While only 5–10 mM 2,6-dcp was needed to shift the E_1° value as shown in Figure 1, much higher concentrations were needed for the weaker acids (0.2–0.5 M were needed for phenol itself). From the shift in the E_1° value, one could estimate the concentration of substituted phenol needed to ensure that most of the reduced product is in the Fe(OEP) (HNO) form. These calculations guided us in the determination of the substituted phenol concentration to be used in this work. Most of the work in this report involved the use of 2,6-dcp, but other phenols were also used to minimize spectral overlap in some experiments (e.g., 2,3-dcp in some of the FTIR experiments or deuterated phenols in the NMR).

Table 1. pK_a Values for Selected Phenols

compound	**pK_a**
2,6-dichlorophenol	6.79
2,3-dichlorophenol	7.76
3,5-dichlorophenol	8.18
phenol	10.00

Visible Spectroelectrochemistry

To obtain spectroscopic evidence of the protonated nitroxyl, the visible spectroelectrochemistry of Fe(OEP) (NO) in THF was carried out (Figure 2A). The results were consistent with previous studies,[29,30] with minimal changes observed in the Soret region, and a new band at 540 nm. The experiment was then repeated in the presence of 20 mM 2,6-dichlorophenol (dcp) (Figure 2B and 2C). Figure 2B shows the first 91 s of the experiment. The Soret band was slightly red-shifted and broadened, and small but reproducible changes were observed in the Q-band region. After 91 s, a new Soret band at 402 nm and a

new band in the Q-band region at 552 nm were observed. Analysis of the data using evolving factor analysis[31] showed clearly that there were three species present during the electrolysis (Figure S2). Deconvolution of the spectra was straightforward as the initial and final spectra could be obtained from the data. The spectra of the three species are shown in Figure S3. The first spectrum was due to the starting complex, Fe(OEP) (NO). Neither of the remaining two spectra in Figure S3 corresponded to Fe(OEP) $(NO)^-$, indicating that the reaction with phenol was fast on the spectroelectrochemical time scale. At this point, we will tentatively assign the second spectrum to Fe(OEP) (HNO) (3), and the third spectrum to Fe(OEP)(H_2NOH) (4), based on the previous work.[24]

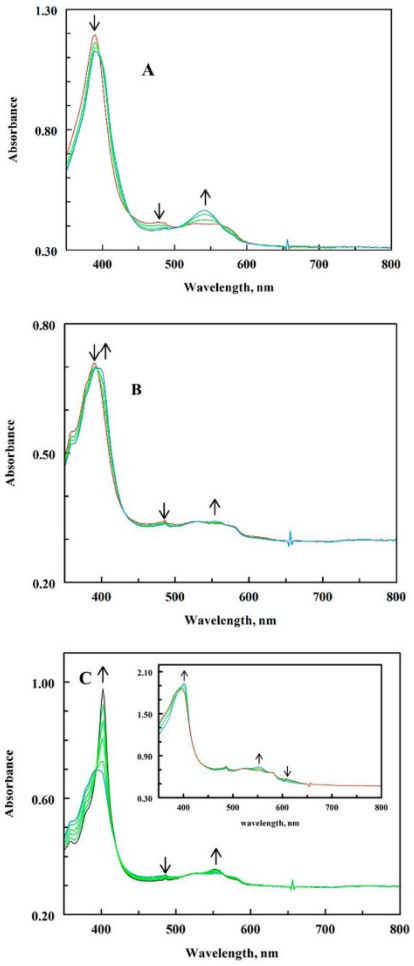

Figure 3. Visible spectra of Fe(OEP) (NO) and Fe(OEP) (HNO) in THF, generated chemically and electrochemically. Black trace: 0.022 mM Fe(OEP) (NO). Red trace: Fe(OEP) (HNO) generated spectroelectrochemically. Blue trace: 0.040 mM Fe(OEP) $(NO)^-$ + 10 mM 2,6-dichlorophenol. Green trace: Addition of 20 mM 2,6-dichlorophenolate to solution of Fe(OEP) $(NO)^-$ + 2,6-dichlorophenol.

As was observed in the cyclic voltammetric experiments, the protonation reaction was reversible, and the extent of protonation can be reduced by the addition of phenolate, driving reaction 2 (Scheme 1) to the left. While the protonation reaction between phenol and the iron nitroxyl is fast on the spectroelectrochemical time scale, the reverse reaction was slow as could be seen in the voltammetric data. Using typical scan rates of 1–5 mV/s, no reoxidation was observed at the scan in the spectroelectrochemical scan. In fact, continued reduction of Fe(OEP) (HNO) to species 4 could be

observed at the end of the scan. This indicates that the thermodynamic $E°$ of Fe(OEP) (HNO) to species 4 was equal to or positive of the Fe(OEP) $(NO)^{0/-1}$ wave. However, kinetic factors prevented the multielectron reduction of Fe(OEP) (NO) in the presences of acid at the first wave. To see the effect of phenolate, a cyclic spectroelectrochemical scan was carried out in the presence of 20 mM 2,6-dcp and 50 mM 2,6-dichlorophenolate. Under these conditions, Fe(OEP) (HNO) was the major product, unlike what was observed in the absence of phenolate. Some species 4 was eventually formed during the scan (Figure 2C, insert). A comparison of Figure 2C and its inset showed that species 4 was significantly suppressed in the presence of phenolate. When the potential was held at −0.60 V, the oxidation of species 4 and Fe(OEP) (HNO) back to Fe(OEP) (NO) was observed.

A second set of spectroelectrochemical experiments were carried out by stepping the potential through the first wave, allowing the solution to come to steady state at each potential in the forward scan. At lower potentials and low concentrations of 2,6-dcp, Fe(OEP) (HNO) was the product of the reduction. As the potential was stepped more negatively, species 4 was formed even at lower concentrations of 2,6-dcp. As the concentration of 2,6-dcp was increased, species 4 was formed at progressively lower potentials, so that it was eventually difficult to observe Fe(OEP) (HNO) in the reduction. These results show that species 4 is formed at the second wave, and the waves will merge if the potential scan is slow enough. These results confirm that the two separate waves that were observed in voltammetry were due to kinetic rather than thermodynamic factors.

The final visible spectroscopic experiment was the spectroelectrochemistry of Fe(OEP) (HNO) generated by the one-electron chemical reduction of Fe(OEP) (NO), followed by the addition of a weak acid. The solution was then reduced electrochemically and the visible spectra monitored (Figure 4). The initial spectrum (black trace) was consistent with the Fe(OEP) (HNO) spectrum. Reduction of the complex gave rise to the 402 nm band that was indicative of species 4. The sharp Soret band was most consistent with a ferrous porphyrin species. The cyclic voltammetric and normal pulse polarographic data both showed a multielectron reduction. The spectroelectrochemical data were most consistent with the formation of a ferrous-hydroxylamine complex (reaction 3, Scheme 1), as the potentials were kept positive of the $Fe^{II/I}$ potential, unlike what was done in the previous study[24] (reaction 5, Scheme 1). On the reverse scan, little reoxidation of the complex was observed. If the potential was maintained at −0.20 V, species 4 (Fe(OEP)(H_2NOH)) was slowly oxidized back to Fe(OEP) (NO). This indicates that the Fe–N bond to the ligand remained intact throughout the redox process.

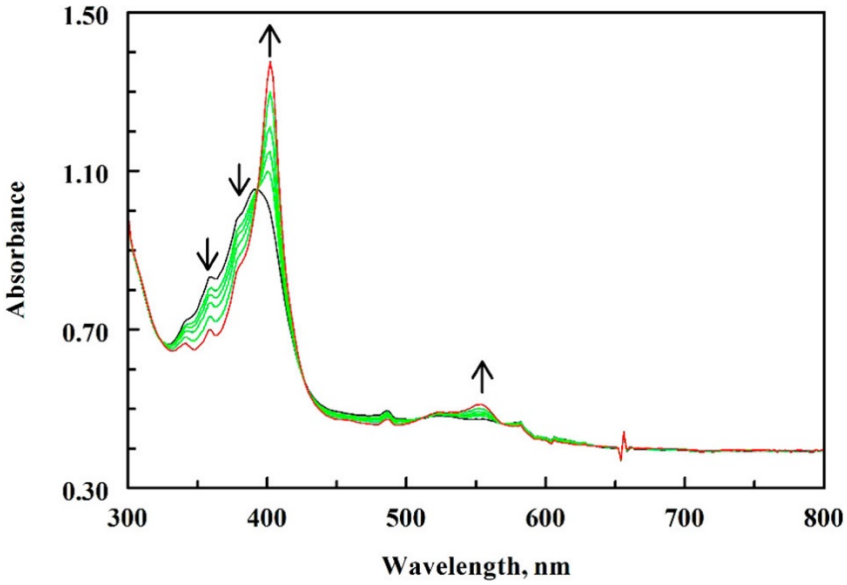

Figure 4. Visible spectroelectrochemistry of 0.15 mM Fe(OEP) (HNO) (generated chemically) in THF with 20 mM 2,6-dcp. A. Initial potential (black), intermediate potentials (green, −0.700, −0.752, −0.816, and −0.900 V), and −1.00 V (red).

There are two reasons that Fe^{II}(OEP)(H_2NOH) continues to be observed during the reverse scan. First, the sluggishness of reaction 2 (Scheme 1), which removes Fe(OEP) (HNO) from the equilibrium. The sluggishness of reaction 2 (Scheme 1) may be due to participation of PhO^- in the rate limiting step. Second, the formation of species 4 is probably controlled by kinetic rather than thermodynamic reasons. Therefore, given enough time, species 4 can be formed at potentials that are more positive than the voltammetric wave. Under these conditions, there was no evidence of the generation for H_2 from the reaction of the phenol with Fe(OEP) $(NO)^-$. If this were occurring, the visible spectrum for Fe(OEP) (NO) would be seen. In fact, the chemically generated Fe(OEP) (HNO) species was stable for hours in the presence of substituted phenols.

^{1}H NMR Spectroscopy

The ^{1}H NMR of Fe(OEP) $(NO)^-$ was obtained in THF-d_8 (Figure 5). The ^{1}H NMR spectrum of Fe(OEP) $(NO)^-$ has been discussed earlier, with the meso-protons appearing at 7.50, 7.59, and 7.77 ppm,[12] with no resonances in the 9–13 ppm region. To this solution, 3,5-dichlorophenol-d_3 was added. New resonances were now observed at 9.3 and 12.6 ppm, and the meso-protons shifted to 7.90, 7.78, and 7.76 ppm. Irradiation at the 12.6 ppm led to an attenuation of the 9.3 ppm resonance, indicating that these two protons were linked by an exchange reaction. In addition, the two resonances were temperature dependent, and shifted toward each other as the temperature changed. Repetition of the NMR experiment with 3,5-dichlorophenol-d_4 yielded no resonances around 12.6 ppm. To the Fe(OEP) $(NO)^-$/3,5-dcp solution, 3,5-dichlorophenolate was then added. After the addition, the resonance at 12.6 ppm disappeared, and the meso-resonances of the OEP ligand reappeared at the position observed for Fe(OEP) $(NO)^-$. DFT calculations for Fe(OEP) (HNO) using the m06 functional predicted a value of 12.2 ppm for the ligand proton. Previous studies showed that the proton in HNO in Fe(OEP) (HNO)(5-MeIm) was 14.0 ppm.[19] The small upfield shift in this case may be due to the lack of trans-coordination, as well as to hydrogen bonding between the complex and the excess phenol. No coupling between ^{15}N (from

Fe(OEP)($H^{15}NO$)) and ligand proton was observed, probably because of rapid proton exchange in the presence of the excess acid.

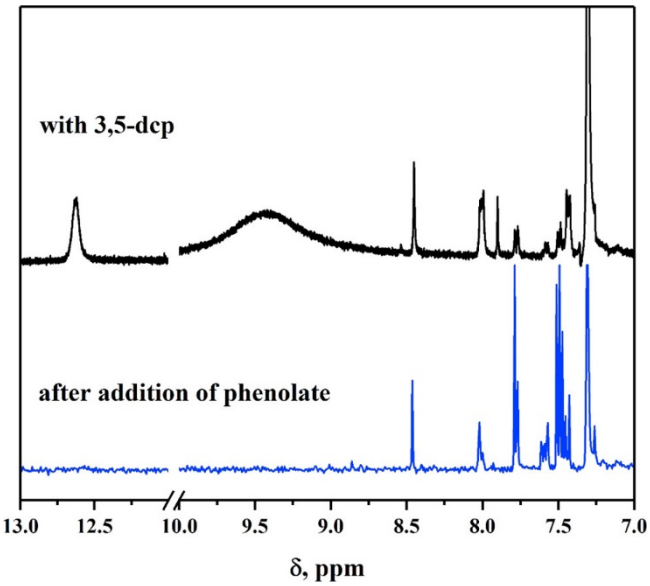

Figure 5. ^{1}H NMR of 7 mM Fe(OEP)(^{15}NO)$^{-}$ in THF. Black trace: Fe(OEP)(^{15}NO)$^{-}$ in the presence of 16 mM 3,5-dichlorphenol-d_3. Blue trace: Solution from blue trace after the addition of 20 mM 3,5-dichlorophenolate-d_3.

Infrared Spectroelectrochemistry

The FTIR spectroelectrochemistry of Fe(OEP) (NO) in THF has already been reported.[28] The ν_{NO} for Fe(OEP) $(NO)^{-}$ was found at 1440 cm^{-1}, which shifted to 1424 cm^{-1} for ^{15}NO. The FTIR spectroelectrochemical spectrum for Fe(OEP) $(NO)^{-}$ is shown in Figure 6A (black trace). In addition to the 1440 cm^{-1} band, a strong band was also observed at 1385 and 1345 cm^{-1}. These bands were identified by DFT calculations to be primarily porphyrin core vibrations with significant coupling to the NO moiety. When Fe(OEP)(^{15}NO) was used, the 1345 cm^{-1} band was downshifted by 2 cm^{-1}. The coupling probably was the source of the increased strength of this band.

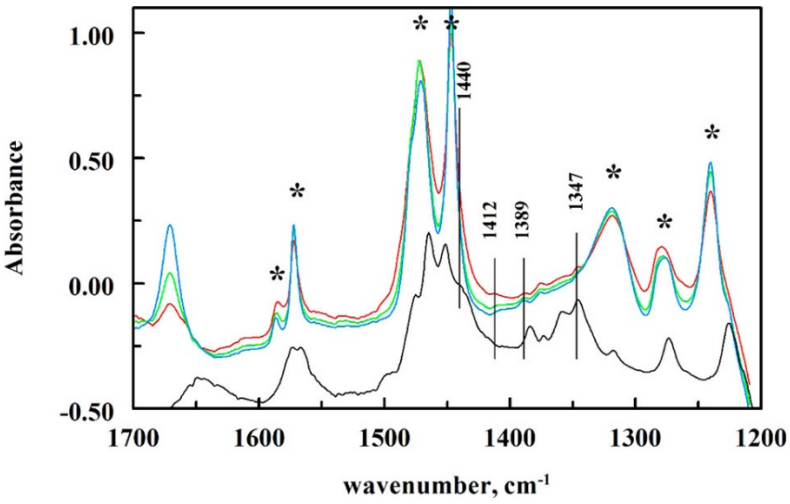

Figure 6. FTIR spectroelectrochemistry of 5.6 mM Fe(OEP) (NO) in THF, after subtraction of the solvent background. Fe(OEP) $(NO)^{-}$ in the absence of 2,6-dcp (black); Fe(OEP) $(NO)^{-}$ in the presence of 2,6-dcp: Initial

spectrum (blue), after 650 s of electrolysis (green), after 1030 s of electrolysis (red). Asterisk (*) indicates 2,6-dcp bands. 1440 cm^{-1} band is the ν_{NO} for Fe(OEP) $(NO)^-$; 1347, 1389, and 1412 cm^{-1} were porphyrin bands for Fe(OEP) (HNO).

The FTIR spectroelectrochemistry of Fe(OEP) (NO) in the presence of 8 mM 2,6-dcp was carried out (Figure 6). Notable differences were observed in the spectra of the reduced species in the absence and presence of weak acid. First, the ν_{NO} vibration at 1440 cm^{-1} was not observed in the presence of 2,6-dcp, indicating that most of the Fe(OEP) $(NO)^-$ had reacted, which was consistent with the cyclic voltammetric and visible spectroelectrochemical data. This also indicated that the reaction of the acid with Fe(OEP) $(NO)^-$ was fast on the spectroelectrochemical time scale. While there was moderate overlap between the 2,6-dcp band at 1447 cm^{-1} and the ν_{NO} band, the ν_{NO} should have been observed if Fe(OEP) $(NO)^-$ were present. To confirm this, Fe(OEP)(^{15}NO) was used, and the ν_{NO} band (now at 1424 cm^{-1}) was still not observed. Second, the bands at 1345 and 1385 cm^{-1} were significantly attenuated in the presence of 2,6-dcp due to the lack of coupling with the NO moiety. In addition, the 1385 cm^{-1} was slightly upshifted, and closer to the Fe(OEP) (NO) value. No isotope sensitive bands were observed between 1450 and 1200 cm^{-1} in the reduced spectrum. In the presence of 2,6-dcp, only weak bands due to the porphyrin vibrations were observed. The spectra taken during the electrolysis (Figure 6) showed the almost complete reduction of Fe(OEP) (NO), and the appearance of the bands becaue of the reduced species. In addition to bands in the starting material, a weak band at 1412 cm^{-1} was observed. The spectra obtained at low potentials were identical to the final spectra (except for the absorbance values) which indicated that further reduction of Fe(OEP) (HNO) to species 4 did not occur.

The FTIR spectroelectrochemistry of Fe(OEP) (NO) and Fe(OEP)(^{15}NO) in the presence of 10 mM 2,6-dcp showed no isotopically sensitive bands, other than the ν_{NO} band for the starting material. As can be seen in Figure 6, the bands for the reduction product were weak, compared to the Fe(OEP) $(NO)^-$ bands. Chemical reduction of both the ^{na}NO (na = natural abundance) and ^{15}NO complexes gave similar results. Even with the use of 2,3-dcp, which had fewer bands in the 1300–1440 cm^{-1} region, no isotopically sensitive bands were observed. In addition, there was no evidence of the disproportionation of Fe(OEP) (HNO) to Fe(OEP) (NO) and H_2 in the FTIR spectra of the chemical reduced nitrosyl complex. This would have been indicated by an increase in the ν_{NO} band for Fe(OEP) (NO).

To confirm that the Fe–N coordination remained after the electrolysis, the potential was returned to the initial potential, and the potential maintained. As was observed in visible spectroelectrochemistry, the infrared spectrum for Fe(OEP) (NO) slowly reappeared, indicating that there was no loss in nitrogen coordination in the reduced complex. Loss of the HNO group would also have rapidly led to N_2O, which would have been observed in the infrared spectrum. Examination of the region above 2200 cm^{-1} showed that no new band appeared (Figure S4). If N_2O was formed, it should have been observed at 2224 cm^{-1}.[32,33] Similar results were observed for the chemically reduced nitrosyl complex.

The voltammetric and spectroscopic data indicate that the pK_a of Fe(OEP) (HNO) is probably between 7 and 8 given the fact that small stoichiometric excesses of 2,6-dcp led to the formation of Fe(OEP) (HNO). Fe(OEP) (HNO) can be formed readily with other dichlorophenols (Table 1), but at higher concentrations. If phenol itself is used, significant reaction between phenol and Fe(P) $(NO)^-$ was only observed at relatively high concentrations of phenol (greater than 100 mM). The FTIR spectroelectrochemistry at 25 mM phenol, for example, showed the presence of Fe(OEP)(^{15}NO)$^-$ in the spectrum (Figure S5), indicating that there was no reaction at this acid concentration. This indicates that the pK_a of Fe(OEP) (HNO) must

between 8 and 10. This makes Fe(OEP) (HNO) a slightly stronger acid than the nonheme Ru–HNO complex discussed previously.[25]

Previous work[24] has shown that the reduction of Fe(P) $(NO)^-$ to Fe(P) (NH_2OH) involves the Fe(P) $(NH_2O)^+$ intermediate (reactions 2, 4, and 5, Scheme 1). As was discussed above, this species is, at best, a minor species at equilibrium, and was not directly observed in our work. An alternate formulation of the reactive intermediate that is consistent with the kinetic data would be a strong hydrogen-bonded complex between phenol and Fe(P) (HNO), Fe(P) (HNO) (HOPh). It is not possible based on the current data to distinguish between this complex and Fe(P) $(NH_2O)^+$.

While the second wave is negative of the first wave in the voltammetric studies, the thermodynamic potential may be positive of the first reduction if the concentration of phenol is high enough. This was demonstrated by the fact that Fe(OEP) (NH_2OH) continued to form during the reverse scan. Eventually, the oxidation of Fe(OEP) $(NO)^-$ will shift the equilibrium and regenerate Fe(P) (NO). This regeneration of Fe(P) (NO) from Fe(P) (NH_2OH) has been verified using UV/visible and FTIR spectroelectrochemistry and confirmed the coordination of the N-ligand during the entire redox process.

Previous studies on Fe(OEP) (HNO) and related complexes have involved six- coordinate species, Fe(P) (HNO)(L). As was discussed earlier, Farmer et al.[15] observed a ν_{NO} band for myoglobin-Fe-HNO at 1385 cm^{-1} using resonance Raman spectroscopy. Abucayon et al.[19] observed a band at 1383 cm^{-1} in the infrared, which they ascribed to ν_{NO}. In our work, this band was not observed by either chemical or electrochemical methods. A significant difference between our work and theirs is the coordination number (6 versus 5), which may account for the differences. The DFT calculations for Fe(P) $(NO)^-$/Fe(P) (HNO) species are summarized in Table 2. The 5-coordinate HNO complexes yielded ν_{NO} values that were upshifted from the six-coordinate complexes. In comparing the DFT calculated IR spectra for the 5-coordinate Fe(P) $(NO)^-$ species with the Fe(P) (HNO) complex, protonation always reduced the calculated ν_{NO} values. With the experimental value of ν_{NO} for Fe(OEP) $(NO)^-$ of 1440 cm^{-1}, one would expect the ν_{NO} for Fe(OEP) (HNO) to be less than that value, and should be observable in our experiment. On the other hand, all the DFT methods underestimated the downshift in the ν_{NO} band in the reduction of Fe(OEP) (NO) to Fe(OEP) $(NO)^-$, even though they calculate the ν_{NO} for Fe(OEP) (NO) itself reasonably well. If the accuracy of the Fe(OEP) (HNO) calculation was similar to the Fe(OEP) (NO) value, there might be an upshift in the five-coordinate Fe(OEP) (HNO) ν_{NO} band upon protonation because most of the DFT values for Fe(OEP) (HNO) are greater than 1440 cm^{-1}. This comparison is more difficult for the six-coordinate complexes because Fe(P) $(NO)^-$ does not coordinate N-ligands.[36] As a result, the ν_{NO} band for five-coordinate Fe(P) (HNO) may be in the congested region between 1450 and 1500 cm^{-1}, and thus would be difficult to observe.

Table 2. DFT Calculations of Iron–Porphyrin–NO^-/HNO Complexes

complex	method	ν_{NO} (cm^{-1})[a]	refs
Fe(P) (ImH) (HNO)	B3LYP/BLYP	1544/1416	34
Fe(P) (Im) (HNO)	mPW1PW91	1375	19
Fe(P) (His) (HNO)	mPWVWN	1374	35
Fe(P) (MeIm) (NO)	mPWVWN	1400	20
Fe(OEP) (HNO)/(FeOEP) $(NO)^-$)	bp86	1455	this work
	m06	1516 (1530)	this work
	m06l	1458 (1503)	this work
	mpwvwn	1401 (1483)	this work

aNumbers in parentheses are for the Fe(P) $(NO)^-$ complex

In this work, we have characterized Fe(OEP) (HNO) and Fe(OEP) (NH_2OH) are five-coordinate complexes. It is reasonable though to expect that THF may occupy the sixth coordination site, though there was no direct evidence for this in this work. For example, Fe^{II}(OEP) in THF is known to be a bis-THF complex.[37] Even for ferrous complexes thought to be 5-coordinate (e.g., Fe(P) (CO)), recent evidence shows that the species is generally 6-coordinate in solution.[38] A second possible ligand for Fe(OEP) (HNO) is the phenolate from the formation of the HNO complex. Evidence for the coordination of the complex with phenolate was observed long-term (days) but led to the displacement of HNO. If this occurred during our experiment, the phenolate complex would have been readily seen in the visible spectrum. Finally, addition of excess phenolate led to deprotonation rather than coordination. No evidence of phenolate coordination was observed in the NMR.

Conclusions

The Fe(OEP) (HNO) complex is readily formed from the reaction of Fe(OEP) $(NO)^-$ with chloro-substituted phenols. For phenol, itself, high concentrations (100 mM or more) are needed to observed any reaction voltammetrically. This work shows that protected iron porphyrin structures are not needed to generate a stable Fe(OEP) (HNO) complex if weak enough acids are used. Previous work[24] has implicated a Fe(OEP)$(H_2NO)^+$ species as an intermediate in the reduction of Fe(OEP) $(NO)^-$ to Fe(OEP) (NH_2OH). This was based on the second-order dependence for phenol in the rate law. An alternate formulation of the reactive intermediate may be a strong hydrogen bonded complex between Fe(OEP) (HNO) and phenol, Fe(OEP) (HNO) (HOPh). The lack of any direct evidence for a second protonation of Fe(OEP) $(NO)^-$ would support this formulation. The spectroelectrochemical data clearly shows the kinetic rather than thermodynamic control for the reduction of Fe(OEP) (HNO) to Fe(OEP)(H_2NOH). Even at potentials well positive of the second voltammetric wave, this reduction can be observed if sufficient time is allowed.

The reoxidation of both Fe(OEP) (HNO) and Fe(OEP)(H_2NOH) was found to be slow. A detailed voltammetric analysis of the oxidation was beyond the scope of this report. The voltammetric data present in Figures 1 and S1 were consistent with a reversible EC mechanism. Oxidation of the Fe(OEP) (HNO) species involves either the oxidation of the iron, which occurs at a much more positive potential, or the oxidation of the HNO species, which leads to an HNO^+ moiety with the proton on the nitrogen. The energetics of the intermediate probably led to a high activation energy. The deprotonation of Fe(P) (HNO) would provide a more facile pathway. Slow deprotonation of HNO in aqueous solution has been reported.[39] This reaction was slow due to a singlet to triplet transition (HNO to NO^-), which does not occur in our reaction due to the coordination of NO^- to Fe(OEP). In addition to Fe(OEP) (HNO), Fe(OEP)(H_2NOH) can also be slowly oxidized back to Fe(OEP) (NO). The kinetics of this process has not been examined. No evidence was observed for the formation of the bis-hydroxylamine complex, Fe(OEP)$(H_2NOH)_2$,[40] which would have also generated Fe^{II}(OEP) from the stoichiometry. This species was not observed in the visible spectrum. The Soret band for Fe(OEP) (NH_2OH) at 402 nm was similar to other ferrous-OEP complexes: Fe(OEP) $(py)_2$, 409 nm;[41] Fe(OEP) (CO) (py), 409 nm;[42] and Fe(OEP)(O_2) (CH_3CN), 410 nm.[42] While these are all six-coordinate complexes, Fe(OEP) (NH_2OH) may be coordinated with THF as was observed for Fe(OEP)(O_2) in acetonitrile.

The reoxidation of hydroxylamine is interesting in that it mimics the hydroxylamine oxidoreductase mechanism. The electrochemical oxidation of an iron-hydroxylamine complex in water leads to a two-electron oxidation to N_2O and H_2O in aqueous solutions,[43] with a Fe-HNO intermediate. The process required the presence of a base. In this case, hydroxylamine was weakly coordinated with iron. Zhang et al.(44) observed a similar oxidation process for a cobalt complex. In our case, the Fe–N bond remains intact, preventing the generation of N_2O from the dimerization of HNO. As a result, the Fe–HNO complex can be oxidized back to Fe–NO. These results are similar to the reaction of the bis-hydroxylamine complex, Fe(P) $(NH_2OH)_2$, with excess hydroxylamine.[40] The overall reaction generated Fe(P) (NO) from the hydroxylamine complex:

$$\mathrm{Fe(P)(NH_2OH)_2} + {}^{1}/_{2}\,\mathrm{NH_2OH} \rightarrow \mathrm{Fe(P)(NO)} + {}^{3}/_{2}\,\mathrm{NH_3} + {}^{3}/_{2}\,\mathrm{H_2O}$$

This reaction provides precedence for the oxidation of hydroxylamine to NO. The stability of this easy to generate Fe-HNO complex should enable researchers to investigate in detail the complex chemistry of coordinated HNO species.

Supporting Information

The Supporting Information is available free of charge on the ACS Publications website at DOI: 10.1021/acs.inorgchem.6b02665.

- Cyclic voltammetry of 0.89 mM Fe(OEP)(NO) in THF with 0.10 M TBAP, forward and reverse evolving factor analysis of the forward scan of the visible spectroelectrochemical reduction of Fe(OEP)(NO) in the presence of 20 mM 2,6-dichlorophenol, visible spectra of Fe(OEP)(NO), Fe(OEP)(HNO), and Fe(OEP)(NH_2OH) in THF, FTIR spectroelectrochemistry of 10 mM Fe(OEP)(NO) in the presence of 10 mM 2,6-dcp, and FTIR spectroelectrochemistry of 3.7 mM Fe(OEP)(^{15}NO) in THF in the absence and presence of 25 mM phenol (PDF)

https://pubs.acs.org/doi/suppl/10.1021/acs.inorgchem.6b02665/suppl_file/ic6b02665_si_001.pdf

References

1. Miranda, K. M. *Coord. Chem. Rev.* **2005**, 249, 433– 455 DOI: 10.1016/j.ccr.2004.08.010
2. Einsle, O.; Messerschmidt, A.; Huber, R.; Kroneck, P. M. H.; Neese, F. *J. Am. Chem. Soc.* **2002**, 124, 11737– 11745 DOI: 10.1021/ja0206487
3. Bykov, D.; Neese, F. *Inorg. Chem.* **2015**, 54, 9303– 9316 DOI: 10.1021/acs.inorgchem.5b01506
4. Daiber, A.; Shoun, H.; Ullrich, V. *J. Inorg. Biochem.* **2005**, 99, 185– 193 DOI: 10.1016/j.jinorgbio.2004.09.018
5. Averill, B. A. *Chem. Rev.* **1996**, 96, 2951– 2964 DOI: 10.1021/cr950056p
6. Cabail, M. Z.; Kostera, J.; Pacheco, A. A. *Inorg. Chem.* **2005**, 44, 225– 231 DOI: 10.1021/ic048822a
7. Shiro, Y.; Fujii, M.; Iizuka, T.; Adachi, S.; Tsukamoto, K.; Nakahara, K.; Shoun, H. *J. Biol. Chem.* **1995**, 270, 1617– 1623 DOI: 10.1074/jbc.270.4.1617
8. Lehnert, N.; Praneeth, V. K. K.; Paulat, F. *J. Comput. Chem.* **2006**, 27, 1338– 1351 DOI: 10.1002/jcc.20400
9. Riplinger, C.; Neese, F. *ChemPhysChem* **2011**, 12, 3192– 3203 DOI: 10.1002/cphc.201100523
10. Farmer, P. J.; Sulc, F. *J. Inorg. Biochem.* **2005**, 99, 166– 184 DOI: 10.1016/j.jinorgbio.2004.11.005
11. Speelman, A. L.; Lehnert, N. *Acc. Chem. Res.* **2014**, 47, 1106– 1116 DOI: 10.1021/ar400256u

12. Kundakarla, N.; Lindeman, S.; Rahman, M. H.; Ryan, M. D. *Inorg. Chem.* **2016**, 55, 2070– 5 DOI: 10.1021/acs.inorgchem.5b02384
13. Lin, R.; Farmer, P. J. *J. Am. Chem. Soc.* **2000**, 122, 2393– 2394 DOI: 10.1021/ja994079n
14. Sulc, F.; Fleischer, E.; Farmer, P. J.; Ma, D. J.; La Mar, G. N. *JBIC, J. Biol. Inorg. Chem.* **2003**, 8, 348– 352 DOI: 10.1007/s00775-002-0422-7
15. Immoos, C. E.; Sulc, F.; Farmer, P. J.; Czarnecki, K.; Bocian, D. F.; Levina, A.; Aitken, J. B.; Armstrong, R. S.; Lay, P. A. *J. Am. Chem. Soc.* **2005**, 127, 814– 815 DOI: 10.1021/ja0433727
16. Lee, J.; Richter-Addo, G. B. *J. Inorg. Biochem.* **2004**, 98, 1247– 1250 DOI: 10.1016/j.jinorgbio.2004.04.005
17. Czarnecki, K.; Kincaid, J. R. *J. Raman Spectrosc.* **2012**, 43, 1343– 1345 DOI: 10.1002/jrs.4046
18. Goodrich, L. E.; Roy, S.; Alp, E. E.; Zhao, J.; Hu, M. Y.; Lehnert, N. *Inorg. Chem.* **2013**, 52, 7766– 7780 DOI: 10.1021/ic400977h
19. Abucayon, E. G.; Khade, R. L.; Powell, D. R.; Zhang, Y.; Richter-Addo, G. B. *J. Am. Chem. Soc.* **2016**, 138, 104– 107 DOI: 10.1021/jacs.5b12008
20. Ling, Y.; Mills, C.; Weber, R.; Yang, L.; Zhang, Y. *J. Am. Chem. Soc.* **2010**, 132, 1583– 1591 DOI: 10.1021/ja907342s
21. Conradie, J.; Ghosh, A. *J. Phys. Chem. B* **2016**, 120, 4972– 4979 DOI: 10.1021/acs.jpcb.6b04983
22. Doctorovich, F.; Bikiel, D. E.; Pellegrino, J.; Suárez, S. A.; Martí, M. A. *Acc. Chem. Res.* **2014**, 47, 2907– 2916 DOI: 10.1021/ar500153c
23. Choi, I.-K.; Liu, Y.; Feng, D.; Paeng, K. J.; Ryan, M. D. *Inorg. Chem.* **1991**, 30, 1832– 1839 DOI: 10.1021/ic00008a028
24. Liu, Y. M.; Ryan, M. D. *J. Electroanal. Chem.* **1994**, 368, 209– 219 DOI: 10.1016/0022-0728(93)03101-T
25. Codesido, N. O.; Weyhermüller, T.; Olabe, J. A.; Slep, L. D. *Inorg. Chem.* **2014**, 53, 981– 997 DOI: 10.1021/ic402448p
26. Kumar, M. R.; Pervitsky, D.; Chen, L.; Poulos, T. L.; Kundu, S.; Hargrove, M. S.; Rivera, E. J.; Diaz, A. D.; Colón, J. L.; Farmer, P. J. *Biochemistry* **2009**, 48, 5018– 5025 DOI: 10.1021/bi900122r
27. Choi, I.-K.; Liu, Y. M.; Wei, Z.; Ryan, M. D. *Inorg. Chem.* **1997**, 36, 3113– 3118 DOI: 10.1021/ic9605783
28. Wei, Z.; Ryan, M. D. *Inorg. Chem.* **2010**, 49, 6948– 6954 DOI: 10.1021/ic100614h
29. Liu, Y. M.; DeSilva, C.; Ryan, M. D. *Inorg. Chim. Acta* **1997**, 258, 247– 255 DOI: 10.1016/S0020-1693(96)05547-8
30. Lançon, D.; Kadish, K. M. *J. Am. Chem. Soc.* **1983**, 105, 5610– 5617 DOI: 10.1021/ja00355a014
31. Keesey, R. L.; Ryan, M. D. *Anal. Chem.* **1999**, 71, 1744– 1752 DOI: 10.1021/ac981079h
32. Martirosyan, G. G.; Azizyan, A. S.; Kurtikyan, T. S.; Ford, P. C. *Inorg. Chem.* **2006**, 45, 4079– 4087 DOI: 10.1021/ic051824q
33. Matsumura, H.; Hayashi, T.; Chakraborty, S.; Lu, Y.; Moënne-Loccoz, P. *J. Am. Chem. Soc.* **2014**, 136, 2420– 2431 DOI: 10.1021/ja410542z
34. Linder, D. P.; Rodgers, K. R. *Inorg. Chem.* **2005**, 44, 8259– 8264 DOI: 10.1021/ic0504745
35. Yang, L.; Ling, Y.; Zhang, Y. *J. Am. Chem. Soc.* **2011**, 133, 13814– 13817 DOI: 10.1021/ja204072j
36. Choi, I.-K.; Ryan, M. D. *Inorg. Chim. Acta* **1988**, 153, 25– 30 DOI: 10.1016/S0020-1693(00)83352-6
37. Kobayashi, H.; Yanagawa, Y. *Bull. Chem. Soc. Jpn.* **1972**, 45, 450– 456 DOI: 10.1246/bcsj.45.450
38. Linder, D. P.; Silvernail, N. J.; Barabanschikov, A.; Zhao, J.; Alp, E. E.; Sturhahn, W.; Sage, J. T.; Scheidt, W. R.; Rodgers, K. R. *J. Am. Chem. Soc.* **2014**, 136, 9818– 9821 DOI: 10.1021/ja503191z

39. Shafirovich, V.; Lymar, S. V. *Proc. Natl. Acad. Sci. U. S. A.* **2002**, 99, 7340– 7345 DOI: 10.1073/pnas.112202099
40. Feng, D.; Ryan, M. D. *Inorg. Chem.* **1987**, 26, 2480– 2483 DOI: 10.1021/ic00262a028
41. Dolphin, D.; Sams, J. R.; Tsin, T. B.; Wong, K. L. *J. Am. Chem. Soc.* **1976**, 98, 6970– 6975 DOI: 10.1021/ja00438a037
42. Welborn, C.; Dolphin, D.; James, B. R. *J. Am. Chem. Soc.* **1981**, 103, 2869– 2871 DOI: 10.1021/ja00400a067
43. Zagal, J.; Villar, E.; Ureta-Zanartu, S. *J. Electroanal. Chem. Interfacial Electrochem.* **1982**, 135, 343– 347 DOI: 10.1016/0368-1874(82)85133-2
44. Zhang, J.; Tse, Y.-H.; Pietro, W. J.; Lever, A. B. P. *J. Electroanal. Chem.* **1996**, 406, 203– 211 DOI: 10.1016/0022-0728(95)04454-X